

Tube Wave removal from vertical seismic profiling (VSP) surveys

Dariusz Nadri

CSIRO Earth Science
& Resource Engineering
PO Box 1130, Bentley
WA, 6102, Australia
Dariusz.Nadri@csiro.au

Milovan Urosevic

Curtin University
Department of Exploration Geophysics
GPO Box U1987, Perth,
WA, 6151, Australia
M.urosevic@curtin.edu.au

Paul Wilkes

CSIRO Earth Science
& Resource Engineering
PO Box 1130, Bentley
WA, 6102, Australia
Paul.Wilkes@csiro.au

Mehdi Asgharzadeh

Curtin University
Department of Exploration Geophysics
GPO Box U1987, Perth,
WA, 6151, Australia
Mehdi.Asgharzadeh@postgard.curtin.edu.au

SUMMARY

This paper presents a processing workflow to attenuate the strong tube waves from VSP surveys acquired in Perth, Western Australia. An array of 24 hydrophones spaced at 10 metre intervals is attached to a cable run down the borehole. The hydrophones were unclamped, so they record significant amount of the tube waves which entirely mask the upgoing waves. F-K filtering was used for wavefield decomposition of flattened downgoing waves. Linear moveout correction was applied to flatten the tube waves and removed unusual aliased energy due to shot depth variations and hydrophone positioning errors through the F-K filtering. The flattened data were transformed to tau-pi domain using a very narrow window slowness to produce a model of tube waves. An adaptive wavefield subtraction algorithm was used to subtract the tube wave model using a matching filter from the input data. The result was processed through a F-K filter and moderate tau-pi filter to remove the residual undesired energy. After attenuating the multiple energy and true amplitude recovery, pre stack depth migration, a CDP-VSP mapping and stacking were applied to produce CDP equivalent depth and time images.

Key words: VSP, tube waves, wavefield subtraction, wavefield decomposition

INTRODUCTION

Geothermal exploration in urban areas is challenged by the constraint of infrastructure within the built up environment. It is very hard and sometimes impractical to acquire surface seismic data for imaging the subsurface structures. Offset VSP, in particular using very long offsets is a convenient and efficient way to image subsurface structure and stratigraphy. They can have higher resolution than surface seismic data but they may come at the cost of drilling wells and shot holes for VSP. In this example, existing boreholes were used to locate the hydrophone array.

GT Power, a geothermal exploration company based in Perth, has elected to use VSP technology in its exploration permits GEP 8 and GEP 9 to gather data from stratigraphy at depth. Two VSP surveys were commissioned by GT Power and these were carried out by Curtin University in association with the WA Geothermal Centre of Excellence and CSIRO.

Conventional three component clamped geophones deployed either in single or few channels, makes data acquisition slow and expensive. On the other way, multichannel hydrophone arrays can be easily deployed at minimal cost and much faster data acquisition. However there are technical issues with

hydrophone arrays. They are generally unclamped and this causes the entire records to be contaminated with strong tube waves.

In this case history a workflow is presented based on an adaptive wavefield separation to remove the modelled tube waves. F-K filters are used to decompose the wavefield into upgoing and downgoing energy. Linear moveout correction is used to flatten the tube waves and pass them through a very narrow slowness window in tau-pi domain to produce the tube wave model. The result shows the tube waves are extensively attenuated at the minimal cost of losing the upgoing P-wave energy.

SURVEY LOCATION AND ACQUISITION

Two VSP surveys were conducted using two boreholes eleven km apart in Perth, Western Australia. The first borehole used a 1000 metre geothermal borehole at St Hilda's School in Mosman Park. The second survey used a 700 metre water monitoring (Department of Water) borehole in Kensington.

The VSP survey used an array of 24 hydrophones spaced at 10 metre intervals attached to a cable run down the borehole. For the first shot the lowest hydrophone was placed at a depth of 680 metres and top hydrophone at depth 450 metres below ground surface. To reduce the receiver spacing the array was moved upwards by 5 metres, for the second shot. For the third shot the array was moved upward for the length of the array such that the top hydrophone was now at a depth of 220 metres below surface. This pattern was used for all six shots to acquire data for the entire borehole with 5 metre receiver spacing. At each offset location two shot holes were drilled down to 8 metres below water level and cased with 50 mm PVC. 150 grams dynamite was used for each blast below the water level for better energy coupling. Each shot damaged the lowest part of the PVC casing so subsequent shots were located up to 2 metres above the previous shot locations. Three shots were fired from each shot hole resulting in 6 shot gathers in each offset. Sampling rate was kept at 0.5 ms and recording length from 3 to 5 seconds for different offsets. A radio system was used to synchronise the trigger and recording systems. In the second survey, we acquired data in five different offsets in the range from 248 to 2197 metres at different azimuths. In the abstract we present the processing workflow for the offset at 248 metres in the second survey.

PROCESSING

A preliminary QC of the shot gathers show large numbers of tube waves contaminated the entire traces regardless of the source receiver offset. Figure 1 shows six shot gathers sorted in receiver depth. It shows that the upgoing P-wave energy is severely masked by all modes of tube waves. Tube waves are not only reflected from the water level and bottom of the

borehole but also from the geological contrasts close to the borehole. For example at the depth of 150 metres there is a group of tube waves (Figure 1) which are reflected from the boundary of two layers with a big velocity contrast as shown in Figure 2.

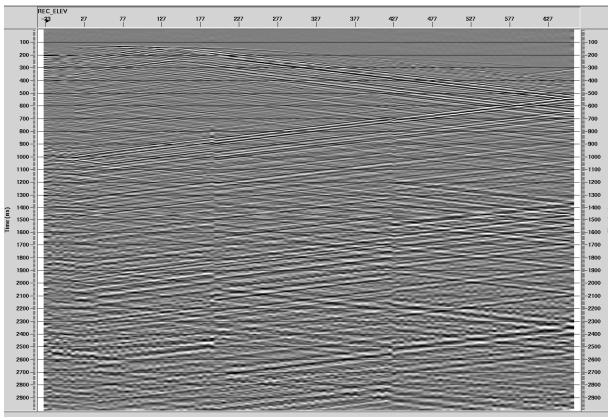


Figure 1. Shot gathers sorted in depth below ground surface. The entire record is contaminated with strong tube waves.

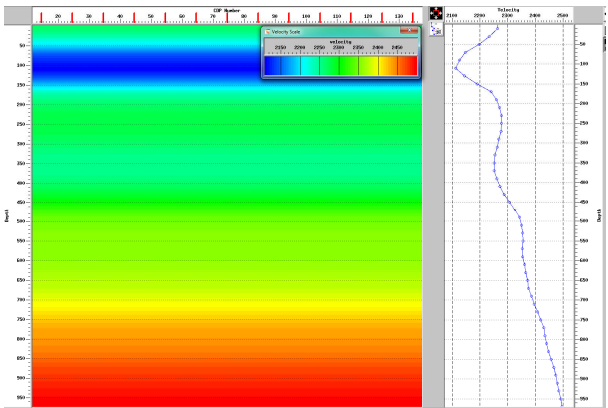


Figure 2. Smoothed interval velocity in depth. The low velocity layer shown in blue colour acts as a reflective boundary for the tube wave.

A second challenge in processing of these datasets, is an unusual aliasing of all the modes in particular tube waves. Figure 3 shows data in T-X and F-K domain from the depth interval of 215 – 445 metres with the 5 metre receiver spacing. The aliased tubes waves, started at very low frequencies and extended up to 280 Hz. This type of aliasing does not appear when we compute the F-K spectrum of data with receiver spacing of 10 metres and from the same shot. The reason is two consecutive shots are not fired from the same depth but with up to two metres difference. Additionally there may be error in positioning the hydrophone array after moving upwards. After merging the two subsequent shot gathers to reduce the receiver spacing to 5 metres, a small shift in the T-X domain cause an aliased comb shape in the F-K domain. This type of aliasing is within the upgoing P-wave energy zone and to remove it we have to sacrifice a small part of the signals. To investigate this issue we created a synthetic model with similar acquisition configuration. We extrapolated the velocity model for the deeper parts from the St Hilda's borehole (700 - 1000 metre depth) and Cockburn 1 well (1-3 km depth) approximately 21 km south west of the Kensington borehole used in survey 2. We used finite difference in elastic

media and a Ricker wavelet with dominant frequency 75 Hz (Figure 4). Shots were located at depths of 30 and 32 metres as per field acquisition geometry and also receivers placed as per field acquisition. We only modelled the body waves and did not model the tube waves. Figure 4 shows the modelled unusual aliasing due to dislocation of the second shot.

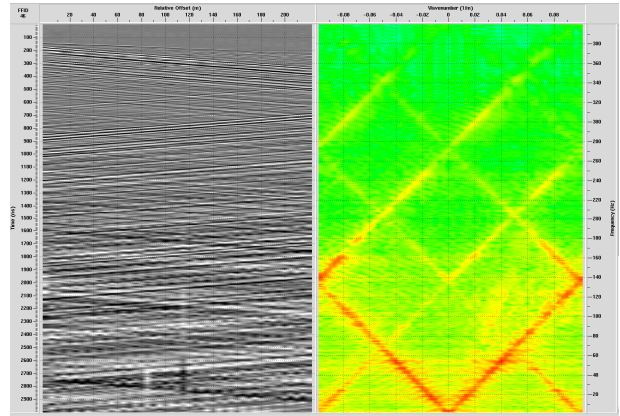


Figure 3. Traces in T-X domain correspond to depth 215 – 445 metres (left panel) and their F-K spectrum (right panel). The unusual aliasing of the tube waves is due to a shift in the location of the next shot.

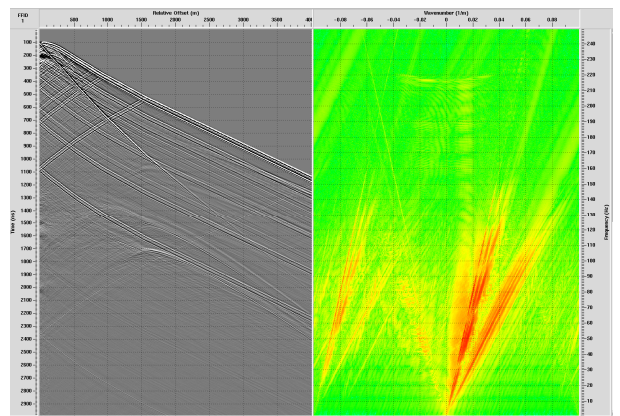


Figure 4. Synthetic seismic in T-X (left panel) using the elastic finite difference modelling by merging the traces from two shots. The unusual aliasing is caused by moving the second shot upwards by 2 metres.

After sorting the data, we assigned the geometry. An Ormsby bandpass filter in the range 12-15-150-180 Hz was used to remove the undesired energy. The first few traces were discarded; these correspond to very shallow depths due to either interference of refracted waves with downgoing P-waves or where refracted waves arrive earlier than the downgoing P-waves. The refracted arrivals are seen as the low energy first arrivals in the first few traces in Figure 1.

Trace equalization was used to correct for the amplitude imbalance due to inconsistent hydrophone coupling. In the next step downgoing p-wave arrivals were removed from the traces before applying bandpass filtering. Where the noise level was high, first arrivals were picked after filtering. The picked first arrivals were used to compute the average velocity and also for flattening the downgoing waves and for true amplitude recovery in the later stages of the processing.

Tube wave removal

In the first attempt to remove the tube waves we flattened the downgoing wave by applying a static correction according to first arrival time. We transform the data to F-K domain and by selecting a window we reject the downgoing P-wave energy and also downgoing tube waves. Any aliased energy with positive slowness was also removed. Figure 5 shows the flattened data in T-X and F-K domain. This window was used to design an operator to attenuate the undesired energy using the F-K filter.

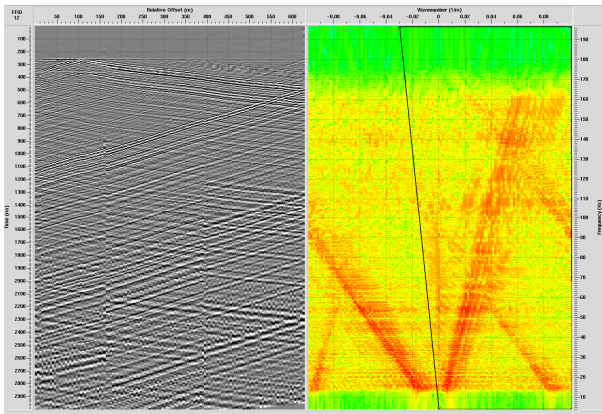


Figure 5. Traces in T-X (left) and F-K (right) domain after flattening the downgoing P-waves. A polygon was used to reject the downgoing energy.

After attenuating the downgoing energy, we unflattened the data by applying an inverse static correction using the first arrival time. We applied linear moveout correction (LMO) to flatten the upgoing tube waves. Figure 6 shows the traces after flattening the tube waves. Mostly the unusual aliased tube waves appear in the negative wavenumber region, but are still seen at positive wavenumbers. The aliased energy with the positive wavenumbers overlaps the upgoing P-wave energy. A narrow window was picked to reject the aliased tube waves. This of course attenuates a small part of the upgoing P-wave energy.

After F-K filtering the aliased energy, the data was transformed to the tau-pi domain using a very narrow slowness (Hardwick, 2011). We used +/- 100 ms/km for inverse tau-pi transform. This removes most of the energies to create a model of the tube waves. Figure 7 shows a model of flattened upgoing tube waves.

In the next step an adaptive wavefield subtraction algorithm (Denisov *et al*, 2006) was used to subtract the flattened F-K filtered upgoing waves and tube wave model. The wavefield subtraction algorithm is a two-step algorithm. First tube waves are predicted and in the second stage, tube waves are adapted to input data with a smoothly varying matching filter via a least square method and are subsequently subtracted. This filter is considered to be a non-stationary adaptive multichannel version of Levinson's algorithm. It requires dividing the tube wave attenuation zones into several time windows, where the signal have similar characteristics. Figure 8 shows the unflattened traces using inverse LMO after adaptive wavefield subtraction. Most of tube wave energy is attenuated.

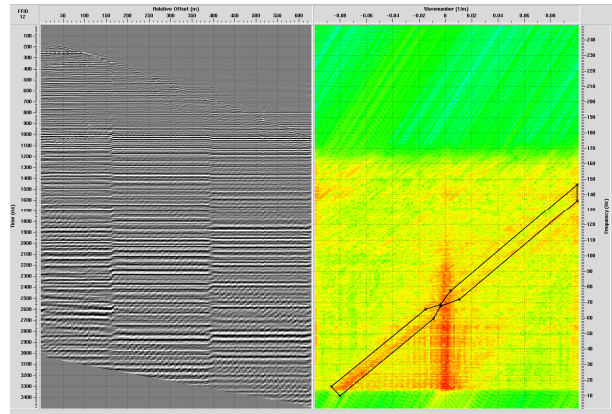


Figure 6. Flattened upgoing tube waves after linear moveout correction. The unusual aliased energy in positive wavenumbers overlaps with upgoing P-waves, hence attenuating a small part of the signals.

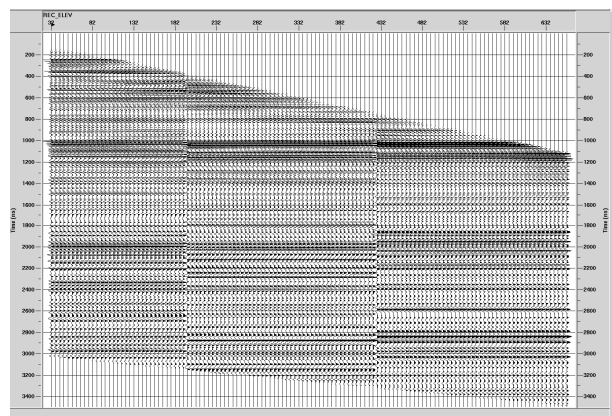


Figure 7. Flattened upgoing tube wave using the linear moveout correction model after F-K and very narrow window tau-pi filtering.

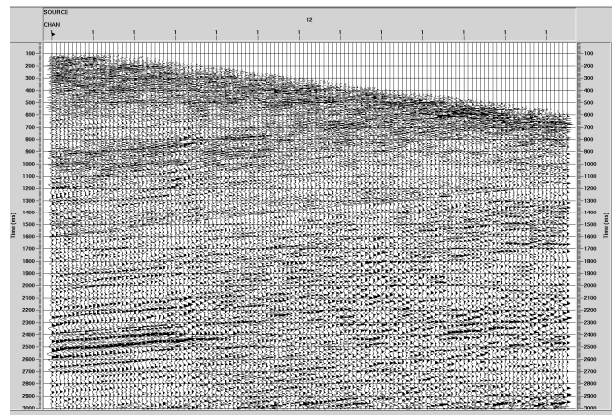


Figure 8. Unflattened upgoing P-waves after adaptive wavefield subtraction and inverse linear moveout correction.

We continued improving the quality of upgoing P-wave energy by passing the data through F-K analysis, removing the residual energy by F-K filter and tau-pi filtering. A window (-500 – 0 ms/km) was used to attenuate the residual tube waves and aliased energy. Figure 9 shows the upgoing P-wave energy after F-K and tau-pi filtering.

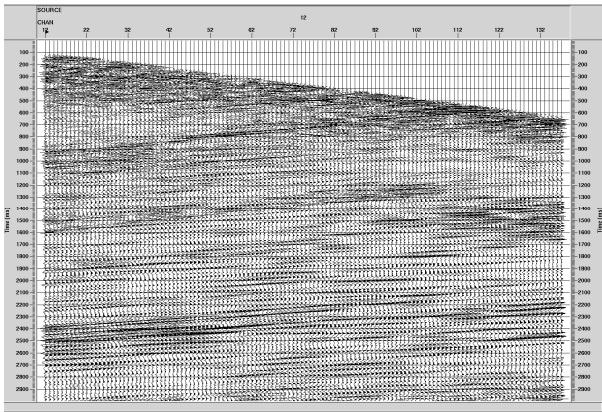


Figure 9. Upgoing P-wave energy after F-K + tau-pi filtering to remove the residual tube waves and aliased energy. Post tube wave removal processing

The conventional VSP deconvolution based on downgoing waves breaks down for offset VSP surveys, in particular in large offsets and where tube waves are dominant. Predictive deconvolution has been shown to be stable and efficient alternative (Sun, *et al*, 2009). Autocorrelation was used to test the different operator lengths and lags for minimum phase predictive deconvolution. Figure 10 shows the autocorrelation of data before and after deconvolution with operator length 200 ms and 7 ms lag. This shows that the relative noise is fairly well attenuated.

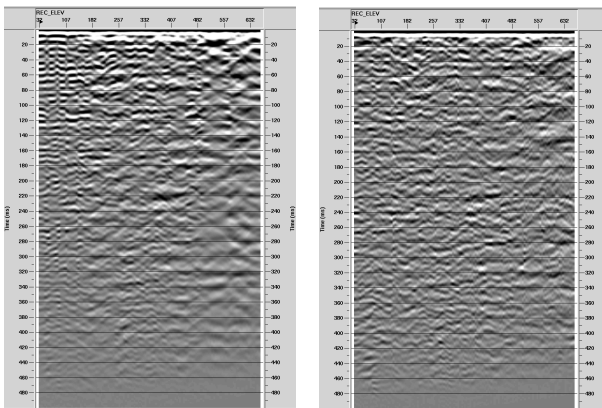


Figure 10. Auto correlation of data before (left) and after (right) minimum phase predictive deconvolution.

Geometrical spreading for true amplitude recovery was applied. The interval velocity from the depth 680 m up to 970 m was extrapolated from the first borehole after reducing the average velocity for 150 m/s to comply with trends seen in the second borehole. Sonic velocities measured in the Cockburn-1 well were used to extrapolate the interval velocities to 3000 metres. These velocities were converted to RMS velocity for geometrical spreading correction and stacking.

CDP-VSP mapping was used to map the upgoing P-waves to the equivalent CDP locations. Ray tracing was used using the interval velocities at 20 metre intervals and used 2.5 metre bins. We stacked the mapped data and migrated using a post stack Kirchhoff time migration algorithm. The migration practically is not necessary in this example, but improves the quality of the image. Figure 11 shows the CDP equivalent post stack time migrated image. Pre stack Kirchhoff depth migration was performed after true amplitude recovery and using interval velocities in depth, as illustrated in Figure 12.

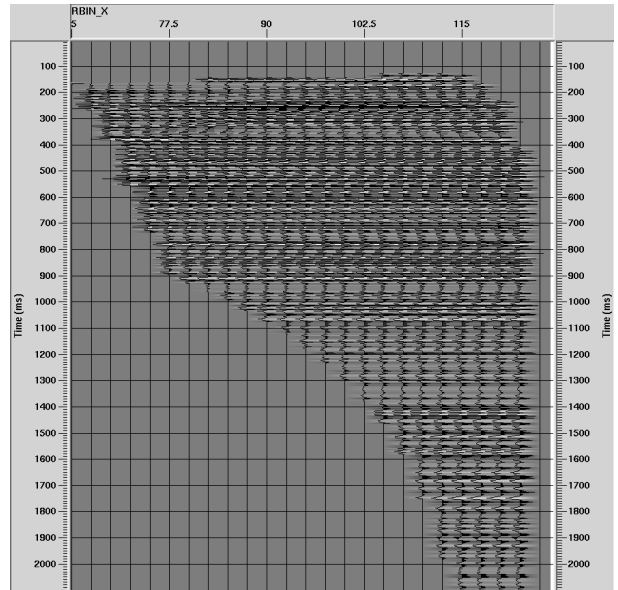


Figure 11. Equivalent CDP image after post stack Kirchhoff time migration.

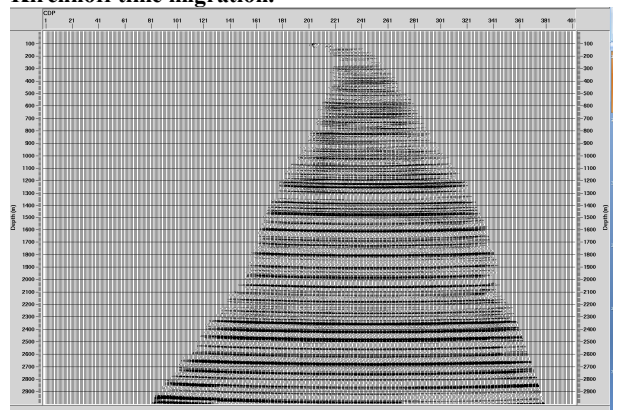


Figure 12. Pre stack Kirchhoff depth migrated image.

CONCLUSIONS

A processing workflow has been designed for the attenuation of strong tube waves which contaminate the offset VSP surveys. The workflow is mainly a combination of F-K filtering and a narrow tau-pi filter to model the tube waves and adaptive wavefield subtraction to remove them.

ACKNOWLEDGMENTS

We thank Hassan Masoomzadeh from TGS for his critical comments during the processing and also Andrew Greenwood and Christian Dupuis from Curtin University for field data acquisition. The authors are grateful for permission by GT Power to use its VSP data in the publication of this research.

REFERENCES

Denisov, M. S., Polubojarinov, M. A., and Finikov, D. B., 2006, Robust methods of adaptive seismic multiple suppression: EAGE St. Petersburg, Expanded Abstracts, European Association of Geoscientists & Engineers, B033.
 Hardwick, A. J., 2011, SMELT - An efficient, flexible method for eliminating multiples: 73rd EAGE Conference and Exhibition, Vienna, Austria, P232.
 Su, X. E., Ling, Y., Gao, J., Lin, J., and Sun, D., 2009, a deconvolution approach using the statistical upgoing waves of zero offset VSP: 71st EAGE Conference & Exhibition, Amsterdam, The Netherland, P321.